Development of MeV Carbon-ion PIXE

C. Chaiwai[1,*], L.D. Yu[1,2,*], U. Tippawan[1]

[1] *Plasma and Beam Physics Research Facility, Department of Physics and Materials Science, Faculty of Science, Chiang Mai University, Chiang Mai 50200, Thailand*
[2] *Thailand Center of Excellence in Physics, Commission on Higher Education, 328 Si Ayutthaya Road, Bangkok 10400, Thailand*

**: Corresponding authors:*
Emails: chicharito_manred001@hotmail.co.th (C. Chaiwai), yuld@thep-center.org (L.D. Yu)

Abstract

In development of MeV heavy-ion particle induced X-ray emission (PIXE) technology which has been demonstrated to be superior to conventional light proton PIXE owing to larger cross sections, MeV carbon-ion PIXE was tested and studied for availability and cross sections. The relatively low ion energy range around 1 MeV for C-ion PIXE had never been investigated before. In the work, C-ion PIXE at ion energy around 1 MeV was firstly tested and demonstrated to be available at our 1.7-MV tandem accelerator and its beam line. In measurement of the cross sections for the MeV C-ion PIXE, 0.8, 1.0 and 1.2 MeV C-ion beams were applied to analyze materials of Si, Fe, Cu, Zn and Au and the spectra were compared with spectra of 1.0- and 2.0-MeV proton PIXE. Results showed that at the same low ion energy of 1 MeV, C-ion PIXE yields were significantly higher by orders than those of proton PIXE which were actually negligible, demonstrating the former significantly more sensitive than the latter. With the 2-MeV proton PIXE cross sections used as the reference, the MeV C-ion PIXE cross sections were calculated. An interesting trend of the cross section against the atomic number *Z* showed that the cross sections of MeV C-ion PIXE compared with those of proton PIXE for the analyzed materials had a transition around Cu. For lower *Z* the former was higher than the latter, while for higher *Z* the former was lower than the latter, indicating MeV C-ion PIXE more sensitive in detecting lower-*Z* elements. Detailed experimental and calculating methods as well as discussions are reported in the presentation.

Introduction

Particle Induced X-ray Emission (PIXE) is an important and routinely used ion beam analysis technique. PIXE was developed initially with using light proton beam but heavy ion PIXE [1,2] later came into the researchers' vision owing to advantages such as larger ion-atom interaction cross section and stopping cross section which eventually led to higher detecting sensitivity [3]. The heavy-ion PIXE technique has been applied to analyze not only solid metals [4] but also particularly biological soft materials [5].

It is well known that proton PIXE conventionally applies proton beams of ion energy higher than 2 MeV so that induced X-ray emission can be possible. With using heavy ion beam for PIXE, the scattering or interaction cross section between the incident ions and the target atoms is increased owing to the increased ion mass, but on the other hand the ion velocity is decreased if the ion energy of both proton and heavy ion is the same to reduce the ionization cross section which depends mostly on the ion velocity [6]. Now we are having two heavy ion beam conditions to choose in order to operate applicable PIXE. One is using higher energy heavy ion beams to keep the same ion velocity with the lower energy proton beam. For carbon ion beam, since the carbon mass is 12 times that of proton, the C-ion beam energy should then be 12 times that of the proton beam. If a standard PIXE of proton beam uses energy of, for example, 2 MeV, the C-ion beam energy is then 24 MeV. Actually some studies using several-tens-MeV or MeV multiply-charged heavy ion beams including C-ion beams have been carried out for PIXE analysis [e.g. 7-9]. The other is using relatively lower energy heavy ion beams so that the interaction cross section can still increase. For the first condition, certainly a high-energy accelerator or more powerful beam line is needed. However, for a resources-limited laboratory, this is not feasible. It turns out for us to choose the second condition. Then, the research question that challenges us is at how low energy of C-ion beam PIXE is still available and what the PIXE cross sections are for the lower-energy C-

ion beams. Based on the technical capabilities of our 1.7-MV tandem accelerator beam line, the energy of C-ion beams was selected to be in the range of around 1 MeV. This is of great significance since this lower energy range of C-ion beams used for PIXE analysis might have never been tested before by any group.

Materials and Methods

Availability tests of C-ion PIXE and MeV proton PIXE

First, C-ion PIXE was tested for its availability at our accelerator and its beam line. As our 1.7-MV tandem accelerator and its beam line (Fig. 1) had been normally applied for proton PIXE analysis, all components of the facility system were fitted to operation of 2-MeV proton beam. With the capability limitation of the mass analyzing magnet at the beam line, it was impossible to bend C-ion beam at energy similar to that of operated proton beams. After the calculation and test it was realized that the maximum energy for C-ion beam was 1.4 MeV. On the other hand, for comparison, proton PIXE would also be operated at the energy the same as the C-ion PIXE. After test it was found that the minimum proton beam energy for PIXE was 0.9 MeV due to the fact that 0.8-MeV proton beam current was immeasurable or zero. The currents of both proton and C-ion beams were measured at the bare sample holder made from aluminium. Although the beam currents measured were not real since no standard secondary electron suppressor was applied, relative values were enough for a comparison to calculate the cross sections.

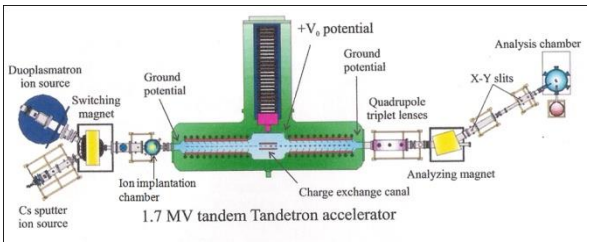

Figure 1. Schematic diagram of the 1.7-MV tandem Tandetron accelerator and its beam line at Chiang Mai University. The beam-bending capability of the mass analyzing magnet after the accelerator and before the analysis chamber regulates the C-ion beam energy.

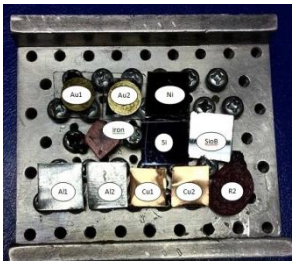

Figure 2. Photograph of some target samples mounted on the sample stage (size: ~ 6cm × 5cm) for PIXE analysis.

Measurements of C-ion PIXE and proton PIXE spectra

C-ion beams at 0.8, 1.0 and 1.2 MeV were applied at the 1.7-MV Tandetron tandem accelerator of our laboratory for PIXE spectrum measurements of target materials of pure (industrial scale) Au, Cu, Fe, Si and Zn, etc. Samples were prepared by cutting and polishing in a disk shape of 1 cm^2 in area and 1 mm in thickness (thus thick samples) and mounted on a sample stage in the target chamber (Fig. 2). The beam spot size was about 2 mm in diameter when focused by the quadrupole triplet lens and finally 1 mm at the sample when controlled by beam entrance apertures. The sample stage was electrically isolated from the chamber. Two permanent magnets were placed in parallel in front of the sample stage as a secondary electrons suppressor, in order to have an accurate measurement of the charge. Characteristic X-rays were detected by a Si(Li) detector kept at an angle of 120^o relative to the beam direction. A mylar foil (74 μm thickness with 0.38% relative hole area) was placed in front of the Si(Li) detector in order to protect the detector from scatterd high-energy-ions damaging and high-rate X-ray counting. The active area of the detector was 30 mm^2. The Si(Li) detector calibration was performed using the X-rays of a ^{109}Cd radioactive source. The energy resolution of the detection system was estimated from the FWHM of the Fe K_α peak at 6.4 keV to be 180 ± 10 eV. An electronic scheme, consisting of preamplifier, amplifier and multichannel analyser (MCA), was used to acquisit spectra. The concentration of each element was determined from the spectrum by using version 2.0 of the Guelph PIXE software package GUPIXWIN. In the PIXE measurement calibration, SRMs (standard reference materials) SRM 610 Trace Elements in Glass Matrix [10] were analyzed as a quality control. The measurement demonstrated the accuracy of the experimental setup to be within ±10%. The beam current at the target was typically about a few nA and the spectral data acquisition time was 1,000 seconds per spectrum for all spectra. For the same target materials, proton PIXE at energy 1.0, 1.2 and 2.0 MeV was also operated for comparison, while 0.8-MeV proton PIXE was demonstrated impossible.

Calculation of C-ion PIXE cross sections

Obtaining of C-ion PIXE cross sections was based on measured PIXE yields. The PIXE yield should be

$$Y \propto N \Delta x \, (It/eA) \, A \, \Omega \, \varepsilon \, \sigma(E, S_i, S_t, X) \, \theta(\theta_i, \theta_d) \quad [11],$$

where N is the atomic number density of target in cm^{-3}, Δx is the ion range or penetration depth, I is the ion beam current in Amp, t is the measurement time in second, e is the charge constant, i.e. 1.6×10^{-19} C, A is the beam area in cm^2, i.e. It/eA is the beam fluence or intensity in cm^{-2} and $(It/eA)A$ is the number of incident ions, Ω is the detector solid angle, calculated from (detector area)/(distance between the target center and the detector)^2, ε is the detector efficiency, $\sigma(E, S_i, S_t, X)$ is the X-ray emission cross section depending on ion energy E, ion species S_i, target species S_t, and X-ray emitted electron shell X. The yield may also depend on the beam incident angle (θ_i) and the detecting angle (θ_d), i.e. $\theta(\theta_i, \theta_d)$.

If a cross section σ_1 for known conditions, including the ion species, target material, ion energy, beam current and then fluence, the X-ray emitted electron shell, and the detector condition is known, an unknown cross section σ_2 of a target species under the same conditions except the ion beam current or fluence can be obtained by the ratio:

$$Y_1/Y_2 = \Delta x_1/\Delta x_2 \times I_1/I_2 \times \sigma_1/\sigma_2,$$

namely,

$$\sigma_2 = \sigma_1 (I_1/I_2) / (Y_1/Y_2) = \sigma_1 (\Delta x_1/\Delta x_2) (I_1Y_2)/(I_2Y_1), \quad (1)$$

where actually $\sigma_1 = \sigma_1(E, S_{i1}, S_t, X)$ and $\sigma_2 = \sigma_2(E, S_{i2}, S_t, X)$. Δx can be calculated from popular ion range programs, such as SRIM [12] and PROFILE [13].

There have been mature theories (e.g. [14]) and computer codes (e.g. Geant4 [15]) to calculate the X-ray emission cross section particularly for proton beam irradiation and data of the proton-induced X-ray emission cross sections can also be found in plenty of literatures. Therefore, in calculation of the C-ion PIXE cross sections, normally 2-MeV proton PIXE cross sections were used as a reference.

Results and Discussion

Measurement of ion beam currents

The measured C-ion and proton beam currents at the sample holder as a function of ion energy are shown in Fig. 3. The proton beam current was nearly linearly increased with the ion energy but it was immeasurable or zero at 0.8 MeV. The C-ion beam current was similar with the proton beam current at energy around 1 MeV but from 1.2 MeV it suddenly increased drastically till 1.4 MeV, beyond which it stopped, indicating that the analyzing magnet reached its maximum beam-bending capacity. The measured beam currents told us which ion beam was available and thus what PIXE analysis was possible.

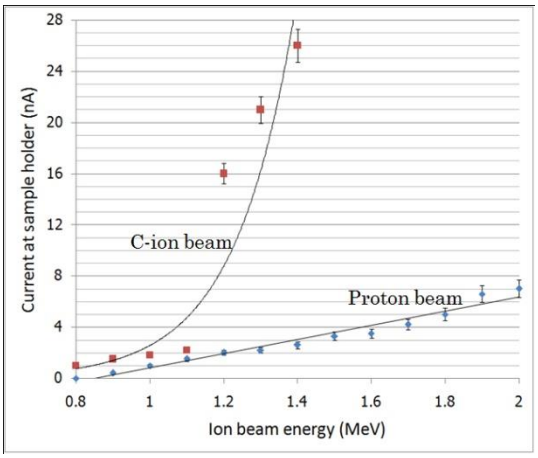

Figure 3. C-ion and proton beam currents at the sample holder as a function of ion energy. The curve and line are only guide lines.

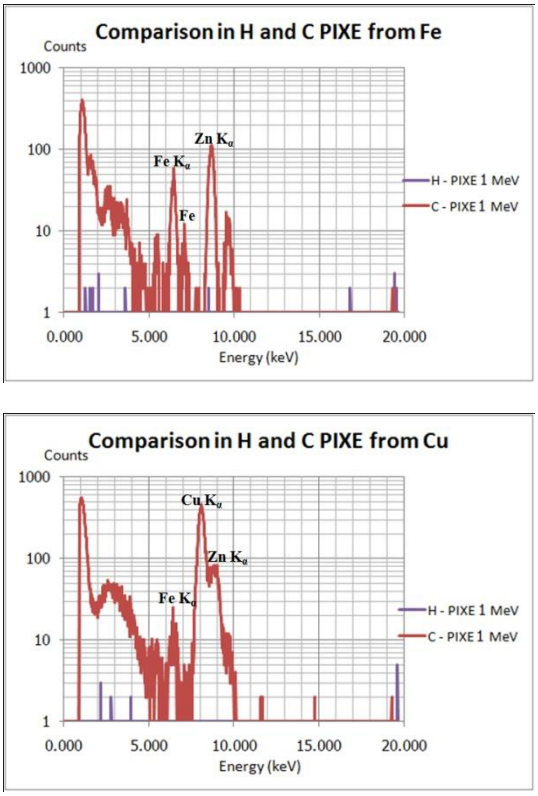

Figure 4. 1-MeV C-ion PIXE spectra from Fe and Cu, compared with the 1-MeV proton PIXE spectra.

Availability of MeV C-ion PIXE

After MeV C-ion beam current was obtained, the MeV C-ion PIXE was tested and spectra were measured as shown in Fig. 4. The spectra shown in the figure clearly demonstrate that MeV C-ion PIXE works. Compared with the proton PIXE spectra using the same ion energy of 1 MeV, the 1-MeV C-ion PIXE yield is significantly higher by orders than the 1-MeV proton PIXE yield which is actually negligible.

MeV C-ion PIXE spectra, compared with standard proton PIXE spectra

Since 1-MeV proton PIXE seemed almost not working, MeV C-ion PIXE spectra were compared with standard 2-MeV proton PIXE spectra, as shown in Fig. 5, for investigation on the cross sections of MeV C-ion PIXE. It is seen that for certain materials the 1-MeV C-ion PIXE spectra are comparable with 2-MeV proton PIXE spectra after subtracting the latter's background. This also tells that the background of the 1-MeV C-ion PIXE spectra is obviously lower than that of 2-MeV proton PIXE spectra. This is believed to be due to less deceleration of ions and electrons which would cause Bremsstrahlung and less secondary irradiation effect from the lower-energy C-ion PIXE. Differences in the yield of characteristic X-ray emission between the two spectra would be applied to calculation of the cross section of the 1-MeV C-ion PIXE as described later in next part.

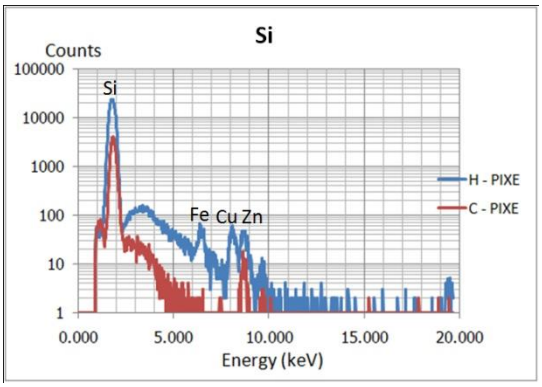

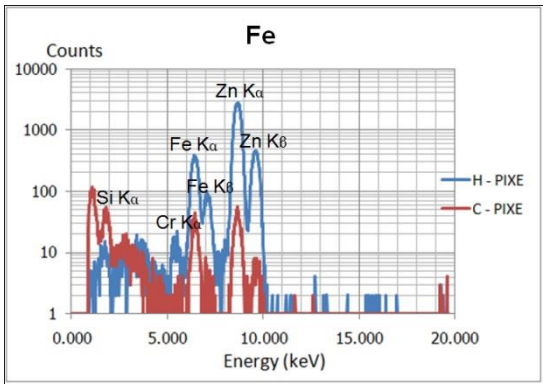

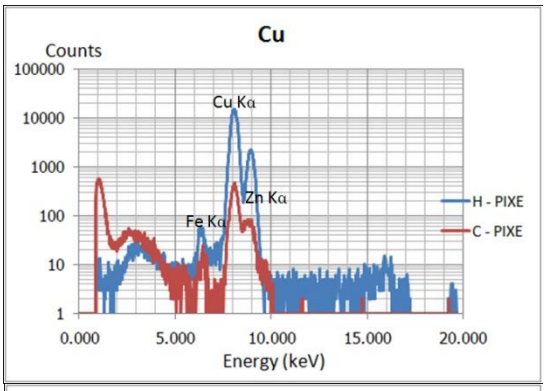

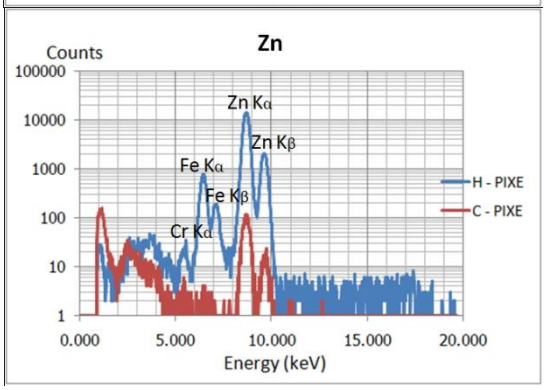

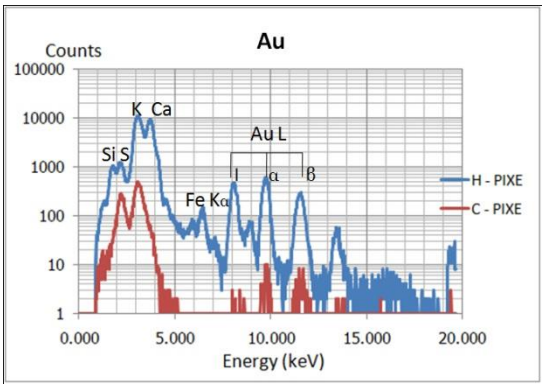

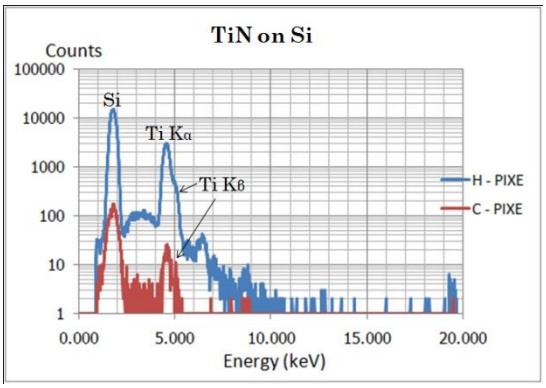

Figure 5. 1-MeV C-ion PIXE spectra compared with 2-MeV proton PIXE spectra from various materials, e.g. Si, Fe, Cu, Zn, Au and TiN thin film on Si.

Calculation of MeV C-ion PIXE cross sections, compared with 2-MeV proton PIXE cross sections

Formula (1) was used to calculate the 1-MeV C-ion PIXE cross sections with the reference of the 2-MeV proton PIXE cross section. For example, let us calculate the cross section for Fe K_α line. The cross section of 2-MeV PIXE is known $\sigma_1 \sim 220$ b for Fe K_α from literatures (e.g. [16]). Ion ranges were calculated from programs (e.g. [12,13]) to be $\Delta x_1 \sim 18{,}400$ nm for 2 MeV proton in Fe and $\Delta x_2 \sim 783$ nm for 1 MeV C ion in Fe, and hence $\Delta x_1/\Delta x_2 \sim 25$. The current ratio is $I_1/I_2 \sim 7/2$ obtained from the current measurement as shown above. The yield ratio is $Y_2/Y_1 \sim 50/400=1/8$, obtained from Fe K_α peaks in the two spectra as shown in Fig. 5. Therefore, the cross section for Fe K_α induced by 1-MeV C-ion beam is $\sigma_2 \sim 10.5$ $\sigma_1 \sim 2310$ b. Fig. 6 shows the calculated 1-MeV C-ion PIXE cross sections for various materials tested and also a comparison with the 2-MeV proton PIXE cross sections.

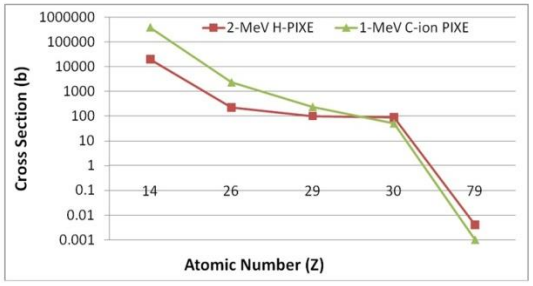

(a)

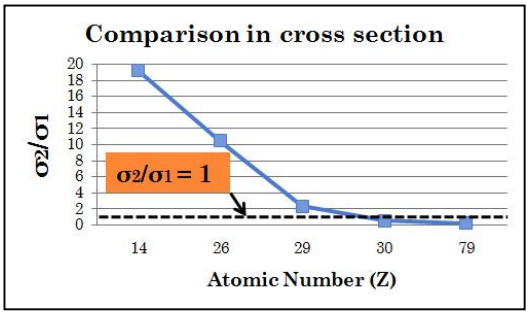

(b)

Figure 6. Calculated PIXE cross sections for K_α lines from 1-MeV C-ion PIXE compared with 2-MeV proton PIXE at target materials of Si, Fe, Cu, Zn and Au, except Au for which the X-ray is L_α line. (a) The cross sections. (b) Comparison in the cross section between 1-MeV C-ion PIXE and 2-MeV proton PIXE by the ratio between the former and the latter.

From the result a trend is noticed. The 1-MeV C-ion PIXE cross sections are higher than those of 2-MeV proton PIXE for elements with lower Z than Cu but lower than those of 2-MeV proton PIXE for elements with higher Z than Zn. Therefore, there is a transition around Cu and Zn. This indicates the MeV C-ion PIXE more sensitive in detecting lower Z elements. For the lower Z elements, the cross sections of MeV C-ion PIXE could be more than ten times those of 2-MeV proton PIXE.

Discussion

The result on low-velocity C-ion PIXE working implies mechanisms involved in the MeV C-ion PIXE probably different from that of standard MeV proton PIXE.

"The relative importance of the various interaction processes between the ion and the target medium depends mostly on the ion velocity and ion charges of the ion and target atoms" [6]. If the ion energy is taken as 1 MeV, the proton and C-ion velocities are $v_H \sim 1.4 \times 10^7$ m/s = 1.4×10^9 cm/s, and $v_C \sim 4 \times 10^6$ m/s = 4×10^8 cm/s, respectively. The Bohr velocity of an electron in the innermost orbit of a hydrogen atom is $v_0 \sim 2.2 \times 10^8$ cm/s. Comparing the ion velocity v_1 with $v_0 Z_1^{2/3}$ for estimating the effective charge of the ion using (for heavy ions, i.e. $Z > Z_{He}$) $Z^*/Z = 1 - \exp[-0.92 v_1/(v_0 Z_1^{2/3})]$, we have

for proton, $Z_1 = 1$, $v_0 Z_1^{2/3} = v_0 = 2.2 \times 10^8$ cm/s, so $v_H > v_0 Z_1^{2/3}$, $Z^* = Z_1 = 1$, but

for C ion, $Z_1 = 6$, $v_0 Z_1^{2/3} \sim 3.3 v_0 \sim 7.3 \times 10^8$ cm/s, $v_C < v_0 Z_1^{2/3}$ and $Z^*/Z \sim 0.4$.

This means that if the ion energy is kept the same, e.g. 1 MeV, a proton is fully stripped to a bare nucleus, while a C ion is not fully stripped or partially stripped by 40%. This turns out that in the two cases, the physics involved in the ionization process is quite different. The electronic interactions are composed of two contributions: (1) close collisions with large momentum transfers, where the particle approaches within the electronic orbits, and (2) distant collisions with small momentum transfers, where the particle is outside the orbits [6]. In the case of proton, it is the first contribution dominated, while in the case of C ion, both contributions exist. Moreover, the fast proton spends less time in the vicinity of the target atom and thus interacts with the atom, whereas the slow C ion spends more time in interaction with the atom, therefore the cross section of the former is smaller than that of the latter.

Conclusions

Our investigation and results on MeV C-ion PIXE clearly demonstrated that low-velocity MeV C-ion PIXE worked, but it could be in different mechanism from that of standard proton PIXE; at the same lower ion energy of 1 MeV, C-ion PIXE was superior to proton PIXE, which was actually impossible; and 1-MeV C-ion PIXE was comparable to 2-MeV proton PIXE particularly for certain materials. The 1-MeV C-ion PIXE cross sections were calculated with reference of 2-MeV proton PIXE based on measured spectral yields, showing an interesting trend which indicated a transition around Cu-Zn, for lower Z elements than Cu the former higher than the latter, while for higher Z elements than Zn the former lower than the latter. The lower-energy C-ion PIXE showed some advantages. It had

considerably higher sensitivity than proton PIXE at the same ion-beam energy owing to larger cross sections. It was comparable to higher-energy proton PIXE but with lower background (Bremsstrahlung) and noises due to less deceleration of ions and electrons and less secondary irradiation effect than higher-energy proton PIXE. It was more sensitive in low-*Z* element detection owing to larger interaction cross sections, so better for biological or organic material analysis. Because of the low energy feature, it was available to resources-limited laboratories in developing countries, and also beneficial to power saving.

Acknowledgments

The work has been supported by the Coordinated Research Projects (CRP) of International Atomic Energy Agency (IAEA), the Chiang Mai University, Thailand, and the Thailand Center of Excellence in Physics.

References

1. M. Uda, O. Benka, K. Fuwa, K. Maeda, Y. Sasa, Nucl. Instr. and Meth. B 22 (1987) 5.
2. M. Terasawa, Int. J. PIXE 1 (1991) 251.
3. Mikio Takai, Yuji Horino, Yoshiaki Mokuno, Akiyoshi Chayahara, Masato Kiuchi, Kanenaga Fujii, Mamoru Satou, Heavy ion microprobes and their applications, Nuclear Instruments and Methods in Physics Research B 77 (1993) 8–16.
4. Yoshiaki Mokuno, Yuji Horino, Akiyoshi Chayahara, Masato Kiuchi, Kanenaga Fujii, Mamoru Satou, Mikio Takai, Application of MeV heavy ion microprobes for PIXE measurements, Nuclear Instruments and Methods in Physics Research B 77 (1993) 128–131.
5. Yuji Horino, Yoshiaki Mokuno, Atsushi Kinomura, Kanenaga Fujii, Microanalysis of human nails by PIXE measurement using heavy ion microprobes, International Journal of PIXE 2 (1992) 299.
6. M. Nastasi, J.W. Mayer and J.K. Hirvonen, Ion-Solid Interactions: Fundamentals and Applications, Cambridge University Press, Cambridge, 1996, p. 99.
7. T. Tadić, D. Dujmić, M. Jaksˇić, V. Valković, C. Manfredotti, Application of MeV carbon ions for PIXE measurements in silicon and high-Tc superconductors, Nuclear Instruments and Methods in Physics Research Section B 109 (1996) 580-583.
8. Ts. Amartaivan, K. Ishii, H. Yamazaki, S. Matsuyama, A.Suzuki, T.Yamaguchi, S.Abe, K.Inomata and Y.Watanabe, PIXE Analysis using 70 MeV Carbons, Proceedings of the 10th International Conference on Particle Induced X-ray Emission and its Analytical Applications, Portorož, Slovenia, June 4-8, 2004. 823.1-823.3.
9. Joonsup Lee, Rainer Siegele, Zeljko Pastuovic, Mark J. Hackett, Nicholas H. Hunt, Georges E. Grau, David D. Cohen, Peter A. Lay, Light and heavy ion beam analysis of thin biological sections, Nuclear Inst. and Methods in Physics Research B 306 (2013) 129-133.
10. National Institute of Standards and Technology, 2005, http://www.eeel.nist.gov/oles/oles_forensic_srms.html.
11. Geoff Grime, Ion Beam Analysis II: Proton or Particle Induced X-ray Emission (PIXE), http://www.spirit-ion.eu/tl_files/spirit_ion/files/Training%20course/Analysis%20II.pdf.
12. J.F. Ziegler, Particles Interactions with Matter, www.srim.org, 2013.
13. Implant Sciences, PROFILE CODE, Wakefield, MA, USA, 1992.
14. Jizhong Zhang, Principle of PIXE, in H.D. Li (Ed.), Applications of Nuclear Technology in Materials Science (in Chinese), Science Press, Beijing (1986), p. 96-100.
15. S. Agostinelli, et al. (totally 127 authors), GEANT4 – a simulation toolkit, Nuclear Instruments and Methods in Physics Research A 506 (2003) 250–303.
16. L.C. Tribedi and P.N. Tandon, K-shell ionization cross sections for low-Z elements ($11 \leq Z \leq 22$) by protons in the energy range 0.5 to 2.5 MeV, Phys. Rev. A 45 (1992) 7860, alsoin http://www.iaea.org/inis/collection/NCLCollectionStore/_Public/24/040/24040180.pdf.